Vortex Core Axial Velocity and Vortex Center Position in Tip Leakage Vortex Using Neural Network Model

Mostafa.Y.El-Bakry

Physics Department, Faculty of Science, Benha University, Egypt

Abstract— *This paper presents dependence of the vortex core axial velocity and vortex center position on clearance in a tip leakage vortex (TLV) for different angles using a system of neural networks (NNs) simulation in which the Resilient Propagation (RPROP) algorithm is applied. These studies are simulation of the vortex core axial velocity and vortex center position as a function of clearance at different angles. The system was trained on the available data of the two cases. The trained NN shows a better agreement with that of an experimental data in two cases; vortex core axial velocity and vortex center position.*

Keywords— Neural Networks, Resilient Propagation (RPROP), vortex core axial velocity, vortex center position, clearance.

I. INTRODUCTION

Tip vortices are prevalent in many industrial applications (e.g., air transportation, marine propulsion, wind turbines, hydraulic machines, space rockets). The need to understand and control the dynamics of these flows has driven numerous researches, producing an abundant literature [see Green [1] and Arndt [2] for a review]. From a theoretical point of view, the model of Batchelor [3], valid far downstream of the wing tip, is widely used to describe the structure of the trailing vortex flow. Moore and Saffman [4] developed a more sophisticated model, valid in the intermediate region between the completion of roll-up and the far field, where the Batchelor solution holds. In axial turbomachinery, a leakage flow occurs between the blade tip and the casing, driven by the pressure difference between the blade pressure and suction sides. The vorticity shed by this leakage flow rolls up into the so-called tip leakage vortex (TLV), which is strongly influenced by the vicinity of the wall (confinement). In axial hydraulic machines, cavitation may develop in the core of TLVs, leading sometimes to severe erosion of the runner blades and the casing, as well as an increase in structural vibrations. Farrell and Billet [5] have found that cavitation incipience in an axial pump may be delayed if the tip clearance is set to an optimum value of about 0.2 times the maximum blade thickness. Boulon et al. [6] examined the effect of the clearance size on the tip vortex generated by an elliptical foil in a setup without relative motion between the end wall and the foil. They found, conversely, that the cavitation inception index increases as the gap is reduced, while no tip vortex cavitation was observed in the most confined cases. Similar observations were reported by Gopalan et al. [7] for the case of a cambered hydrofoil in a water tunnel. More recently, Wu et al. [8] and Miorini et al. [9] studied experimentally the internal structure of the TLV within the rotor of an axial waterjet pump using both 2D and stereo-PIV. They observed that the instantaneous TLV structure is composed of unsteady vortex filaments that propagate into the tip regionof the blade passage and roll up into the TLV. They noticed that vortex breakdown could also occur as the TLV migrated toward the pressure side of the neighboring blade, changing drastically the vortex characteristics, as reported by Pasche et al. [10]. The measured velocity fields in these studies were, however, limited to a few tip clearance values. In the specific area of Kaplan turbines, the wake of the distributor guide vanes produces a highly non-uniform pressure field, which leads to repetitive collapses and rebounds of the cavitating tip vortices. Obviously, cavitation erosion depends not only on the vortex strength and core size, but also on its trajectory and how far it stands from solid boundaries. It should be noted that, nowadays, it is still not possible to fairly predict cavitation occurrence in axial turbines, neither from numerical simulations nor from reduced scale model tests. In their attempt to mitigate the cavitation development in axial turbines, engineers commonly implement the so-called anti-cavitation lip, which consist of a simple winglet attached to the tip of the blades. Nevertheless, such a remedy often fails to reduce cavitation erosion, as reported by Roussopoulos and Monkewitz [11] on a simplified case study. Dreyer et. al [12] study the structure and trajectory of a TLV generated at the tip of a fixed 2D hydrofoil experimentally for different confinements and flow parameters. They perform accurate measurements of the velocity field to better understand the underlying physics of vortex confinement.

It is assumed that the mean vortex flow is not fundamentally altered by the end wall motion. they have selected the SPIV technique for the measurement of the 3D velocity field.

In the present study, the data obtained by Dreyer et. al [12] is chosen to be carried out using the neural networks depending on the BP and RPROP algorithms.

Neural networks are widely used for solving many problems in most science problems of linear and non-linear cases [13-15]. Neural network algorithms are always iterative, designed to step by step minimise (targeted minimal error) the difference between the actual output vector of the network and the desired output vector, examples include the Backpropagation (BP) algorithm [16-18], and the Resilient Propagation (RPROP) algorithm [19-21].

BP is the most widely used algorithm for supervised learning with multi-layered feed-forward networks [22], and it is very well known, while the RPROP algorithm is not well known and described in some detail in section 2.1.

The RPROP algorithm was faster than the BP [23-24]. Therefore, the RPROP is chosen to be carried out in this study. The present work offers an efficient neural network that is used to simulate the data of the vortex core axial velocity and vortex center position as a function of clearance at different angles. The following sections provide a brief introduction to NNs, describe the selected NN structure, training data and discuss the results.

II. NEURAL NETWORKS

Neural networks consist of a number of units (neurons) which are connected by weighted links. These units are typically organised in several layers, namely an input layer, one or more hidden layers, and an output layer. The input layer receives an external activation vector, and passes it via weighted connections to the units in the first hidden layer. Figure (1) shows input layer with R elements, one hidden layer with S neurons, and output layer with one element. Each neuron in the network is a simple processing unit that computes its activation $y_i^{(1)}$ with respect to its incoming excitation, the so-called net input net_i:

$$net_i = \sum_{j \in pred(i)} s_i w_{ij} - b_i \qquad (1)$$

Where $pred(i)$ denotes the set of predecessors of unit i, w_{ij} denotes the connection weight from unit j to i unit, and b_i is the unit bias value. The activation of unit i, $y_i^{(1)}$, is computed by passing the net input through a non-liner activation function. The tan-sigmoid function is applied in the proposed work as follows.

$$y_i^{(1)} = f_{tansig}(net_i) = \frac{1}{1+e^{-2net_i}} - 1 \qquad (2)$$

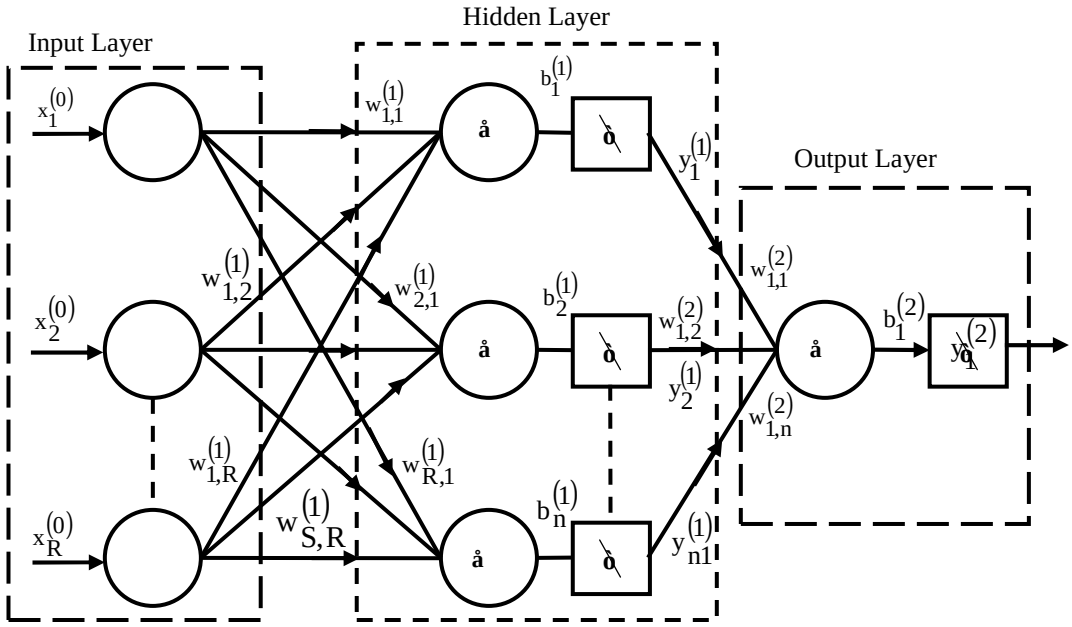

Fig.1: Network Architecture for one hidden layer

2.1 RPROP Algorithm

In the RPROP algorithm, each weight (w_{ij}) is computed by its individual update-value ($D_{ij}^{(t)}$), which determines the size of the weight-update. This adaptive update-value evolves during the learning process based on its local sight on the error function E, according to the following learning-rule [19].

$$\Delta_{ij}^{(t)} = \begin{cases} \eta+ * \Delta_{ij}^{(t-1)}, \text{if } \frac{\partial E^{(t-1)}}{\partial w_{ij}} * \frac{\partial E^{(t)}}{\partial w_{ij}} > 0 \\ \eta- * \Delta_{ij}^{(t-1)}, \text{if } \frac{\partial E^{(t-1)}}{\partial w_{ij}} * \frac{\partial E^{(t)}}{\partial w_{ij}} < 0 \\ \Delta_{ij}^{(t-1)}, \quad \text{else} \end{cases} \quad (3)$$

where $0 < \eta- < 1 < \eta+$

The size of the weight change is exclusively determined by the weight-specific update-value $D_{ij}^{(t)}$. Every time the partial derivative of the corresponding weight changes its sign, the update-value is decreased by the factor η. This indicates that the last update was too big and the algorithm jumped over a local minimum. On the other hand, if the derivative retains its sign the update-value is slightly increased by the factor η in order to accelerate convergence in shallow regions. Once the update-value for each weight is adapted, the weight-update is changed as follows: if the derivative is positive (increasing error) the weight is decreased by its update-value, if the derivative is negative, the update-value is added. Then, the weights are updated as in equation (5) using update-values from equation (4).

$$\Delta_{ij}^{(t)} = \begin{cases} -\Delta_{ij}^{(t)}, \text{if } \frac{\partial E^{(t)}}{\partial w_{ij}} > 0 \\ +\Delta_{ij}^{(t)}, \text{if } \frac{\partial E^{(t)}}{\partial w_{ij}} < 0 \\ 0 \quad , \quad \text{else} \end{cases} \quad (4)$$

$$w_{ij}^{t+1} = w_{ij}^{(t)} + \Delta w_{ij}^{(t)} \quad \text{(Riedmiller and Braun 1993)} \quad (5)$$

As mentioned in the Section 1, the RPROP algorithm was faster than the BP, the main reason for the success using this algorithm is that the size of weight-step is only dependent on the sequence of signs, not on the magnitude of the derivative as showed by Riedmiller and Braun [24]. The RPROP algorithm has fewer parameters that need to be evaluated and promises to provide the same performance as an optimally trained network using the BP algorithm.

2.2 Proposed Algorithm

The studied problem consists of two independent-parts, the first is the vortex core axial velocity as a function of clearance in a tip leakage vortex (TLV) for different angles and the second is the vortex center position as a function of clearance in a tip leakage vortex (TLV) for different angles. Each part contains four groups of data. Each group are chosen as patterns for training and simulation.

Our problem has two inputs (clearance and angle), and single output (vortex core axial velocity) in each part, because there is only one target value associated with each input vector; see figure (2) network (1). We have preferred to use the same neural network architecture in the both vortex core axial velocity and vortex center position see figure (2) network (2).

The RPROP was trained and tested using different parameters, for instance, changing the number of hidden layers, neurons, epochs, and testing the networks. The chosen algorithms were first trained up to 500 epochs for vortex core axial velocity part and 400 epochs for vortex center position. After the training, it was noticed that the RPROP algorithm using three hidden layers was very effective using log-sigmoid transfer function in the hidden layers and a linear transfer function in the output layer.

More hidden layers or neurons require more computations, but allow the network to solve complicated problems. Therefore, we have done many tries to find the best network used low number of hidden layers and neurons. For first network, 1, 2, 3 hidden layers with 12, 13 and 15 neurons are used for solving the vortex core axial velocity problem. The second network 1, 2, 3 hidden layers with 14, 12 and 11 neurons are used for solving the vortex center position problem. We first set up the network with random weights and biases values.

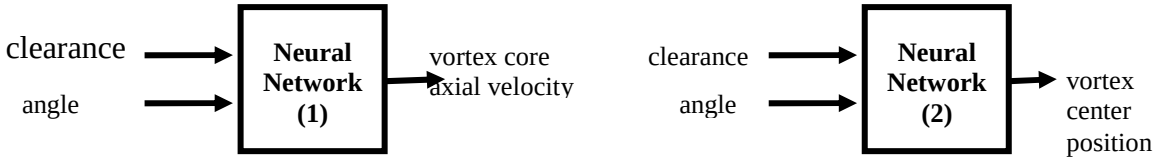

Fig.2: A block diagram modeling

The equation which describe the normalized vortex core axial velocity or vortex center position is discussed in (Appendix A).

III. RESULTS

The above mentioned of proposed neural network were applied and simulated to the data of the vortex core axial velocity or vortex center position as a function of clearance at different angles in a tip leakage vortex (TLV).

The chosen neural network was trained on four cases of different angles for each of the vortex core axial velocity or vortex center position as a function of clearance. These values of the normalized vortex core axial velocity are 3.043 multiplied by 10^{-5} and for vortex center position with clearance 4.929 multiplied by 10^{-5} . The performances of the obtained networks for two cases are shown in figure (3) and Figure (4). Figure (5) shows the neural networks results of the four cases training for normalized vortex core axial velocity with clearance. Figure (6) shows also the neural networks results of the four cases training for vortex center position with clearance. It was observed that these figures illustrate an excellent performance in simulation. These results of the dependence of normalized vortex core axial velocity and vortex center position on clearance at different angles are presented in the figure(5) and figure(6).

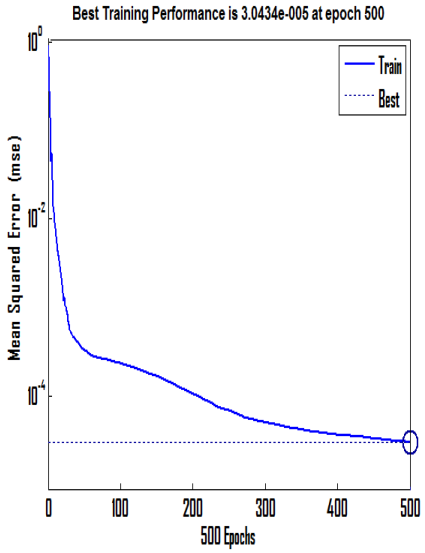

Fig.3: The NN performance for vortex core axial velocity

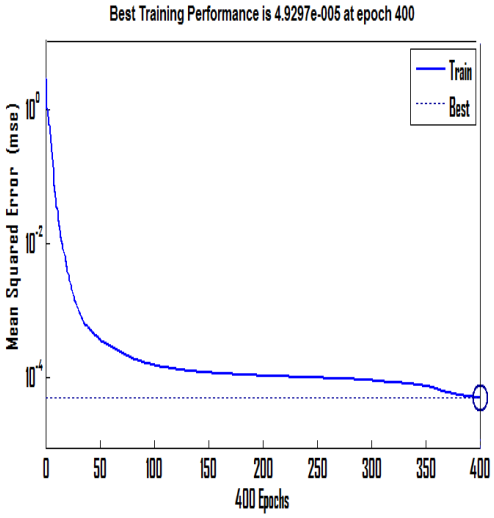

Fig.4: The performance of NN for vortex center position

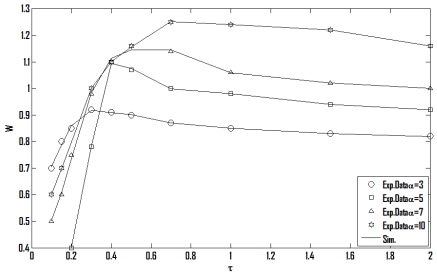

Fig.5: The NN simulation of the vortex core clearance

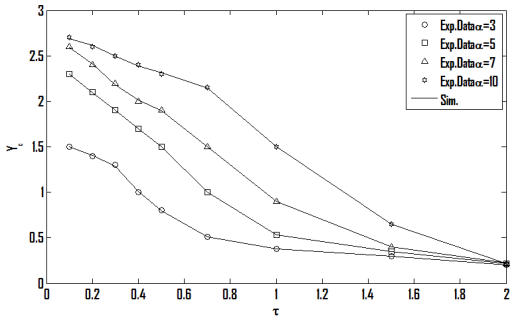

Fig.6:The simulation result of the vortex center axial velocity with position with clearance

IV. CONCLUSION

We have done many tries to find the best network used low number of hidden layers and neurons. It was found that, 1, 2, and 3 hidden layers with 12, 13 and 15 neurons are used for solving the vortex core axial velocity problem and 1, 2 and 3 hidden layers with 14, 12 and 11 neurons are used for solving the vortex center position problem are enough for reaching the optimal solution.

The trained NN using the proposed algorithm shows excellent results matched with the experimental data in the two cases of the vortex core axial velocity and vortex center position problems. The NN technique has been also designed to obtain the one equation which simulate the vortex core axial velocity and vortex center position and matched them effectively. The (NNs) simulation using RPROP algorithm is powerful mechanism for simulation of the vortex core axial velocity and vortex center position on clearance in a tip leakage vortex (TLV) for different angles.

Appendix A

The equation which describe normalized vortex core axial velocity or vortex center position is given by:

W or Y_c =Pureline [net. LW{4,3} logsig(net.LW{3,2} logsig(net.LW{2,1} logsig(net. IW{1,1} A+net. b{1})+net. b{2})+net. b{3})+net. b{4}],

Where,

A = α and τ is the input
net. IW{1,1}: linked weights between the input layer and first hidden layer.
net. LW{2,1}: linked weights between the first hidden layer and the second hidden layer.
net. LW{3,2}: linked weights between the second hidden layer and third layer.
net. LW{4,3}: linked weights between the third hidden layer and output layer.
net . b{1}: is the bias of the first hidden layer.
net . b{2}: is the bias of the second hidden layer.
net . b{3}: is the bias of the third hidden layer.
net. b{4}: the bias of the output layer.

REFERENCES

[1] Green SI, Fluid vortices: fluid mechanics and its applications, vol 30. Springer, Berlin, (1995)
[2] Arndt RE, Cavitation in vortical flows. Annu Rev Fluid Mech. 34(1):143–175, (2002)
[3] Batchelor GK, Axial flow in trailing line vortices. J Fluid Mech 20:645–658. doi: 10.1017/ S0022112064001446, (1964).
[4] Moore DW, Saffman PG, Axial flow in laminar trailing vortices. Proc R Soc Lond Ser A Math Phys Sci 333(1595):491–508, (1973).
[5] Farrell K, Billet M A, correlation of leakage vortex cavitation in axial-flow pumps. J . Fluids Eng 116(3):551–557, (1994).
[6] Boulon O, Callenaere M, Franc JP, Michel JM, An experimental insight into the effect of confinement on tip vortex cavitation of an elliptical hydrofoil. J Fluid Mech 390:1–23, (1999)
[7] Gopalan S, Katz J, Liu HL Effect of gap size on tip leakage cavitation inception, associated noise and flow structure. J Fluids Eng 124(4):994–1004, (2002).
[8] Wu H, Tan D, Miorini RL, Katz J, Three-dimensional flow structures and associated turbulence in the tip region of a waterjet pump rotor blade. Exp Fluids 51(6):1721–1737. doi:10.1007/s00348-011-1189-9 (2011).
[9] Miorini RL, Wu H, Katz J, The internal structure of the tip leakage vortex within the rotor of an axial waterjet pump. J Turbomach 134 (3): 031,018, (2012).
[10] Pasche S, Gallaire F, Dreyer M, Farhat M, Obstacle-induced spiral vortex breakdown. Exp Fluids 55(8):1–11.doi:10.1007/s00348-014-1784-7, (2014).
[11] Roussopoulos K, Monkewitz PA, Measurements of tip vortex characteristics and the effect of an anti-cavitation lip on a model Kaplan turbine blade. Flow Turbul Combust 64(2):119–144, (2000).
[12] Dreyer M, Decaix J, Munch-Alligne C, Farhat M, Mind the gap: a new insight into the tip leakage vortex using stereo-PIV, Exp Fluids 55:1849 DOI 10.1007/s00348-014-1849-7, (2014).
[13] Mostafa Y. El-Bakry, Radial Basis Function Neural Network Model for Mean Velocity and Vorticity of Capillary Flow, International Journal For Numerical Methods In Fluids, Vol. 67:1283–1290 (2011).
[14] Mostafa Y.El-Bakry, D.M.Habashy and Mahmoud Y.El-Bakry, Neural Network Model for Drag coefficient and Nusselt number of square prism placed inside a wind tunnel, International Journal of Scientific & Engineering Research, Vol. 5, Issue 6, June(2014).
[15] Mostafa Y.El-Bakry, D.M.Habashy and Mahmoud Y.El-Bakry, Effect of Particles on Flow Structures in Secondary SedimentationTanks Using Neural Network Model, International Journal of Scientific & Engineering Research, Volume 6, Issue 5, May(2015).
[16] Yi-Chung Hu, and Jung-Fa Tsai, Backpropagation multi-layer perceptron for incomplete pairwise comparison matrices in analytic hierarchy process, Applied Mathematics and Computation, vol. 180, No. 1, pp. 53-62 (2006).
[17] Curry B, Morgan PH, Model selection in Neural Networks: Some difficulties**,** European Journal of Operational Research, vol. 170, No. 2, pp. 567-577 (2006).
[18] Jochen J. Steil**,** Online stability of Backpropagation–decorrelation recurrent learning**,** Neurocomputing, vol. 69, No. 7-9, pp. 642-650 (2006).
[19] Riedmiller, M., Advanced supervised learning in multi-layer perceptrons from Backpropagation to adaptive learning algorithm, Computer Standards & Interfaces, vol. 16, pp. 265-278 (1994).
[20] Christian Igel, and Michael Hüsken, Empirical evaluation of the improved Rprop learning algorithms**,** Neurocomputing, vol. 50, pp. 105-123 (2003).
[21] Carreras E S, Elkissi N, Piau JM, Toussaint F, Nigen S, pressure effects on viscosity and flow stability of polyethylene melts during extrusion, Rheologica Acta, vol. 45, No. 3 pp. 209-222 (2006).
[22] Frasconi P, Gori M, Soda G, Links between LVQ and Backpropagation, Pattern Recognition Letter, vol. 18, pp. 303-310 (1997).
[23] Riedmiller M, Braun H, A direct adaptive method for faster Backpropagation learning: The RPROP algorithm in H. Ruspini, ed., Proc. IEEE Internat. Conf. On Neural Networks (ICNN), San Francisco, pp. 586-591 (1993).
[24] El-Harby A A, Automatic extraction of vector representations of line features from remotely sensed images, PhD Thesis (Keele University, UK), (2001).